

# Synthesis and thermal decomposition of organosilicon hexamine cobalt-containing xerogels

Vladimir V. Semenov,<sup>a</sup> Larisa G. Klapshina,<sup>a</sup> William E. Douglas<sup>b</sup> and Georgii A. Domrachev<sup>\*a</sup>

<sup>a</sup> G. A. Razuvaev Institute of Organometallic Chemistry, Russian Academy of Sciences, 603600 Nizhnii Novgorod, Russian Federation. Fax: +7 312 66 1497; e-mail: klarisa@imoc.sinn.ru

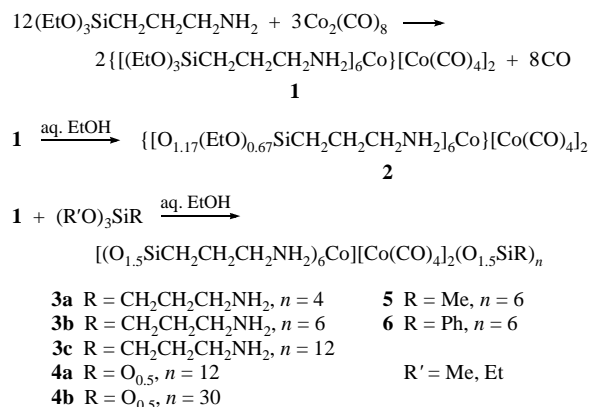
<sup>b</sup> CNRS UMR 5637, Université Montpellier II, 34095 Montpellier Cedex 5, France

10.1070/MC2000v010n04ABEH001221

The treatment of 3-aminopropyltriethoxysilane (APTES) with  $\text{Co}_2(\text{CO})_8$  resulted in hexa(3-aminopropyltriethoxysilane)cobalt(II) bis(tetracarbonylcobaltate) **1**, the co-hydrolysis of which with APTES, tetraethoxysilane,  $\text{MeSi}(\text{OMe})_3$  and  $\text{HO}(\text{Me}_2\text{SiO})_n\text{OH}$  afforded cobalt-containing xerogels or transparent films.

Organosilicon gels are produced by hydrolysis of alkoxide precursors or alkali metal organosilicates.<sup>1–3</sup> Transparent aerogels<sup>4,5</sup> and monolithic glasses<sup>6</sup> can also be obtained. A sol–gel silica host matrix is an excellent medium for organic non-linear optical materials, which improves their optical transparency and mechanical strength and protects the dopant from harmful environments. Indeed, transparent silica glasses containing transition metal atoms are the most promising versatile materials possessing useful electrical, magnetic and optical properties.<sup>6–8</sup> Supported-metal porous materials are of interest to heterogeneous catalysis. Transition metal-containing inorganic–organometallic hybrid materials were described previously.<sup>1–4,9</sup> Here, we consider novel hexamine cobalt-containing silica glasses and powders prepared by the sol–gel method. The method is based on a homomolecular disproportionation reaction of dicobalt octacarbonyl with 3-aminopropyltriethoxysilane (APTES) giving hexa(3-aminopropyltriethoxysilane)cobalt(II) bis(tetracarbonylcobaltate),<sup>†</sup> which was co-hydrolysed with an excess of APTES, tetraethoxysilane (TEOS),  $\text{MeSi}(\text{OMe})_3$  or  $\text{PhSi}(\text{OMe})_3$  (Scheme 1).<sup>‡</sup>

Complex **1** is an oxygen- and moisture-sensitive red liquid soluble in benzene, diethyl ether,  $\text{CHCl}_3$ , and THF and sparingly soluble in hexane. Satisfactory elemental analysis for  $\text{Co}^{2+}$  in complex **1** was obtained by the  $\text{Na}_2\text{S}$  precipitation method.<sup>†</sup> No gel was formed on the hydrolysis of **1** with distilled water. Removal of alcohol from the reaction mixture gives complex **2** (transparent glassy brown granules) containing unreacted ethoxy groups. The addition of an excess of water (10–12%) to a solution of **1** in APTES (the **1**:APTES molar ratios 1:4, 1:6 and 1:12) results in gelation after 10–12 h. Removal of the alcohol and drying of the gel gives lilac non-porous glass-like xerogels of **3a–c**. Co-hydrolysis of **1** with TEOS (the molar ratios 1:12 and 1:30) results in rapid gelation with the formation of chalk-like



Scheme 1

porous gels (**4a** and **4b**). Xerogels **5** and **6** are transparent brown glasses; the gelation occurred after 12–15 h.

The preparation of complex **1** at atmospheric pressure of argon was accompanied by the evolution of only 0.8 mol of CO instead of 8 mol expected (Scheme 1). About 90% CO reacted with amino groups to give amide derivatives. This is confirmed by the appearance of two bands at 1630 (CO) and 1545  $\text{cm}^{-1}$  (NH) in the IR spectrum of the reaction products. The absorption of carbon monoxide in the reaction of primary amines with  $\text{Co}_2(\text{CO})_8$  was observed previously.<sup>10–11</sup> The amide derivatives formed are included in the coordination sphere of  $\text{Co}^{\text{II}}$  together with  $\text{NH}_2$  ligands. However, the reaction of  $\text{Co}_2(\text{CO})_8$  with APTES performed in a vacuum with the removal of CO from the reaction mixture gave complex **1** enriched in  $\text{NH}_2$  ligands.

The IR spectra of **1–6** exhibit bands at 2000–1965 and 1870  $\text{cm}^{-1}$  attributed to the  $[\text{Co}(\text{CO})_4]^-$  anion. All the products exhibit Si–O–Si bands in the region 1140–1000  $\text{cm}^{-1}$ , and amine and/or amide ligand  $\nu_{\text{N–H}}$  absorption bands at 3450–3010  $\text{cm}^{-1}$ . The bands at 1155, 1075, 950 and 775  $\text{cm}^{-1}$  in the spectrum of **1** are attributed to  $\text{Si}(\text{OEt})_3$  fragments. For **2–4**, a broad band in the range 2730–2500  $\text{cm}^{-1}$  indicates the presence of  $-\text{NH}_3^+$ , formed on the hydrolysis of **1** by partial decomposition with the

<sup>†</sup> Compound **1** was prepared by mixing  $\text{Co}_2(\text{CO})_8$  (1.49 g,  $4.35 \times 10^{-3}$  mol) and APTES (3.80 g,  $1.72 \times 10^{-2}$  mol) in a vacuum with continuous stirring, cooling and removal of evolved CO from the reaction mixture for 2 h. The resulting viscous red liquid was washed with hexane; the yield was 3.87 g (78%). <sup>1</sup>H NMR ( $\text{CDCl}_3$ , 100 MHz)  $\delta$ : 0.51 (s, 12H,  $\text{CH}_3\text{Si}$ ), 1.07 (s, 54H,  $\text{MeCH}_2\text{O}$ ), 2.39 (s, 12H,  $\text{CH}_2\text{N}$ ), 3.65 (s, 36H,  $\text{MeCH}_2\text{O}$ ). IR ( $\nu/\text{cm}^{-1}$ ): 3380, 3250, 3120 ( $\text{NH}_2$ ), 1995, 1870, 550 (CO), 1630, 1570 [ $\text{NH}_2$ ,  $\text{NHC}(\text{O})\text{H}$ ], 2950, 2900, 2870, 1470, 1430, 1380, 1358, 1289, 1155, 1075, 950, 775, 465 [ $\text{Si}(\text{CH}_2)_3$ ,  $\text{SiOEt}$ ]. Found (%): C, 42.20; H, 8.17; Co<sup>II</sup>, 3.36; N, 4.73. Calc. for  $\text{C}_{62}\text{H}_{138}\text{Co}_3\text{N}_6\text{O}_{26}\text{Si}_6$  (%): C, 43.07; H, 8.04; Co<sup>II</sup>, 3.41; N, 4.86. Co<sup>II</sup> was determined by the known method<sup>11</sup> in methanol.

Compound **2**, 95% yield. IR ( $\nu/\text{cm}^{-1}$ ): 3380, 3280, 3140 ( $\text{NH}_2$ ), 2700–2500 ( $\text{NH}_3^+$ ), 1990, 1870, 543 (CO), 1630, 1580, 1540 [ $\text{NH}_2$ ,  $\text{NHC}(\text{O})\text{H}$ ], 1150, 950, 780, 460 ( $\text{SiOEt}$ ), 1050 ( $\text{SiOSi}$ ). Found (%): C, 32.80; H, 5.88; N, 6.82. Calc. for  $\text{C}_{34}\text{H}_{68}\text{Co}_3\text{N}_6\text{O}_{21}\text{Si}_6$  (%): C, 32.87; H, 5.52; N, 7.02.

Compound **5**, 92% yield. IR ( $\nu/\text{cm}^{-1}$ ): 3420, 3340, 3250 ( $\text{NH}_2$ ), 2000, 1870, 540 (CO), 1615, 1570, 1530 [ $\text{NH}_2$ ,  $\text{NHC}(\text{O})\text{H}$ ], 1255, 760, 710, [ $\text{Si}(\text{CH}_2)_3$ ,  $\text{SiOEt}$ ,  $\text{SiMe}$ ], 1125, 1025 ( $\text{SiOSi}$ ). Found (%): C, 31.33; H, 5.74; Co, 10.48; N, 4.98. Calc. for  $\text{C}_{44}\text{H}_{96}\text{Co}_3\text{N}_6\text{O}_{29}\text{Si}_{12}$  (%): C, 31.09; H, 5.53; Co, 10.83; N, 4.39.

<sup>‡</sup> Xerogels were prepared by the addition of an excess of water (10–15%) in ethanol to an ethanolic solution of complex **1** and  $(\text{R}'\text{O})_3\text{SiR}$ . Xerogel **7** was obtained by the same method from APTES and TEOS (1:4).

Table 1 Physical properties of xerogels.<sup>a</sup>

Xerogel	Skeletal density/ g cm <sup>-3</sup>	Bulk density/ g cm <sup>-3</sup>	Effective porosity	Effective volume/ cm <sup>3</sup> g <sup>-1</sup>	Surface area/m <sup>2</sup> g <sup>-1</sup>	
					starting xerogel	after heating <sup>b</sup>
<b>2</b>	1.42	1.43	—	—	—	38.8
<b>3a</b>	1.83	1.85	—	—	—	—
<b>3b</b>	1.40	1.46	—	—	—	8.1
<b>4a</b>	1.71	1.49	0.13	0.09	12.5	15.1
<b>4b</b>	1.66	0.69	0.58	0.85	28.4	59.1
<b>7</b>	1.89	0.39	0.79	2.03	35.9	—

<sup>a</sup>The skeletal density (density of the xerogel solid framework only) and bulk density (porous solid density with the pore volume included) were determined by the use of a pycnometer with methanol as the penetrant. <sup>b</sup>Under argon in a closed system at 500 °C.

formation of  $\text{H}[\text{Co}(\text{CO})_4]$ . This hydride is a strong protic acid, which reacts with APTES to give  $-\text{CH}_2\text{NH}_3^+[\text{Co}(\text{CO})_4]^-$  units. Thus, products **2–6** contain, in addition to the main structure  $\{(\text{O}_{1.5}\text{SiCH}_2\text{CH}_2\text{CH}_2\text{NH}_2)_6\text{Co}\}[\text{Co}(\text{CO})_4]_2$ , the structures arising from partial amide substitution  $\{(\text{O}_{1.5}\text{SiCH}_2\text{CH}_2\text{CH}_2\text{NH}_2)_n-[\text{O}_{1.5}\text{SiCH}_2\text{CH}_2\text{CH}_2\text{NHC}(\text{O})\text{H}]_{6-n}\text{Co}\}[\text{Co}(\text{CO})_4]_2$ . Products **2–4** also contain cobalt carbonyl anions neutralised by the ammonium cation  $-\text{CH}_2\text{NH}_3^+$  rather than  $\text{Co}^{2+}$ . If  $\text{MeSi}(\text{OMe})_3$  or  $\text{PhSi}(\text{OMe})_3$  is used in the co-hydrolysis, the IR spectra of the resulting xerogels exhibit bands due to Si–Me (1255 and  $760\text{ cm}^{-1}$ ) or Si–Ph ( $3060\text{--}3000$ ,  $730$  and  $690\text{ cm}^{-1}$ ), respectively, rather than  $-\text{NH}_3^+$  units.

The solid-state  $^{29}\text{Si}$  NMR spectra of the xerogels consist of three broad resonance signals at  $-66$ ,  $-79$  and  $-82\text{ ppm}$ , which correspond to the fragments  $\text{R}(\text{R}'\text{O})_2\text{SiO}$  ( $T_1$ ),  $\text{R}(\text{R}'\text{O})\text{SiO}_2$  ( $T_2$ ) and  $\text{RSiO}_3$  ( $T_3$ ) ( $\text{R} = \text{CH}_2\text{CH}_2\text{CH}_2\text{NH}_2$ , Me, Ph;  $\text{R}' = \text{Et}$ , Me), respectively. Thus, all T-structures that can be formed on hydrolysis of organotrialkoxysilanes are present in the xerogels. The absence of signals in the region from  $-90$  to  $-110\text{ ppm}$  shows the absence of  $\text{SiO}_4$  fragments in the products. Thus, the cleavage of Si–C bonds does not occur during the hydrolysis. Elemental analysis gives the empirical formula  $\{[(\text{EtO})\text{OSiCH}_2\text{CH}_2\text{CH}_2\text{NH}_2]_6\text{Co}\}[\text{Co}(\text{CO})_4]_2[\text{O}_{1.5}\text{SiR}]_n$ .

Table 1 summarises data on the density and porosity of xerogels. The similar skeletal and bulk densities and the absence of a nitrogen desorption peak in the BET data are consistent with the non-porous structure of glass-like products **2**, **3a** and **3b**. The specific surface area of chalk-like xerogels **4a** and **4b** increased with diluting complex **1** by TEOS (the 1:TEOS ratio is 1:12 for **4a** or 1:30 for **4b**). The surface area is maximum for xerogel **7** obtained in the absence of metal complexes.

We examined the thermal decomposition of products **3**, **5** and **6**. Product **3a** remained transparent after thermal treatment at  $150^\circ\text{C}$ , and the IR spectra remained almost unaffected after treatment at  $150\text{--}200^\circ\text{C}$ . However, after heating to  $250^\circ\text{C}$ , the intensities of bands due to CO stretching and deformation vibrations in the cobalt carbonyl anion decreased considerably. A similar effect was observed for the  $\nu_{\text{N-H}}$  bands in the region  $3500\text{--}3100\text{ cm}^{-1}$ . After treatment at  $250^\circ\text{C}$ , no absorption due to  $-\text{NH}_3^+$  appeared in the region  $2800\text{--}2500\text{ cm}^{-1}$ , however, the intensities of the  $\nu_{\text{Si-O-Si}}$  stretching bands at  $1110$  and  $1070\text{ cm}^{-1}$  increased. Pyrolysis at  $200\text{--}250^\circ\text{C}$  gives rise to  $\text{H}_2$ , CO,  $\text{CO}_2$ ,  $\text{NH}_3$ , and saturated and unsaturated hydrocarbons. An increase in the temperature from  $150$  to  $250^\circ\text{C}$  was accompanied by a sharp increase in gas evolution (from  $0.75$  to  $9.2\text{ mol}$ ). After heating to  $150$ ,  $200$  and  $250^\circ\text{C}$ , the ratio  $\text{H}_2\text{:CO:CH}_4$  (determined by gas chromatography on NaX zeolite) was  $27\text{:}73\text{:}0$ ,  $14\text{:}86\text{:}0$  or  $33\text{:}45\text{:}22$ , respectively. Two processes are responsible for hydrogen formation. First, dissociation of  $\text{O}_{1.5}\text{SiCH}_2\text{CH}_2\text{CH}_2\text{NH}_3\text{Co}(\text{CO})_4$  results in  $\text{O}_{1.5}\text{SiCH}_2\text{CH}_2\text{CH}_2\text{NH}_2$  and  $\text{HCo}(\text{CO})_4$  at relatively low temperatures. The cobalt carbonyl hydride formed is converted into  $\text{Co}_2(\text{CO})_8$  and  $\text{H}_2$ . This process is accompanied by the disappearance of the IR absorption of  $-\text{NH}_3^+$ . The second process is the interaction of the  $[\text{Co}(\text{CO})_4]^-$  anion and the intermediate sub-carbonyl Co species with  $\text{NH}_2$  groups at higher temperatures ( $250\text{--}500^\circ\text{C}$ ). Heating to  $500^\circ\text{C}$  leads to complete disappearance of cobalt carbonyl, NH and CH fragments; the IR spectrum exhibited only two bands in the region  $1150\text{--}1000\text{ cm}^{-1}$  corresponding to a siloxane framework. No crystalline phase was formed on pyrolysis at  $150\text{--}$

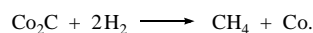
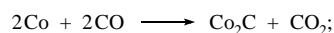
**Table 2** X-ray powder diffraction analysis of pyrolyzed xerogels **5** and **6**.

$T/^\circ\text{C}$	Atmosphere	Compound	Solid phases identified
150	argon	<b>5</b>	amorphous
		<b>6</b>	amorphous
200	argon	<b>5</b>	amorphous
		<b>6</b>	elemental cobalt traces
250	argon	<b>5</b>	$\alpha\text{-Co}$ , $\beta\text{-Co}$ , $\text{Co}_2\text{C}$
		<b>6</b>	$\alpha\text{-Co}$ , $\beta\text{-Co}$ , $\text{Co}_2\text{C}$
600	argon	<b>5</b>	$\alpha\text{-Co}$ , $\beta\text{-Co}$
		<b>6</b>	$\alpha\text{-Co}$ , $\beta\text{-Co}$ , graphite
600	oxygen	<b>5</b>	$\text{Co}_3\text{O}_4$ , $\alpha\text{-Co}$ , $\beta\text{-Co}$
		<b>6</b>	$\text{Co}_3\text{O}_4$ , $\alpha\text{-Co}$ , $\beta\text{-Co}$

**Table 3** Effect of the conditions of thermal treatment on the xerogel surface area.

Compound	Surface area/ $\text{m}^2\text{ g}^{-1}$			
	Starting xerogel	Thermal treatment conditions		
		Argon flow, $600^\circ\text{C}$	Oxygen flow, $600^\circ\text{C}$	Oxygen flow, $1000^\circ\text{C}$
<b>3b</b>	2.0	19	25	31
<b>5</b>	0.4	236	148	90
<b>6</b>	0.3	478	272	228

$250^\circ\text{C}$ . A metallic cobalt phase appeared on treatment at  $500^\circ\text{C}$ . The presence of  $\text{CO}_2$  and  $\text{CH}_4$  in the gas phase may be explained by the following well-known reactions of cobalt:



Two temperature regions can be distinguished in the TGA curves of xerogels **3b**, **5** and **6** (Figure 1), which correspond to the most rapid weight loss between  $100\text{--}300$  and  $300\text{--}500^\circ\text{C}$ . The first region is due to decomposition of cobalt carbonyl groups and the second, to cobalt(II) hexamine groups. The maximum weight loss on heating to  $1200^\circ\text{C}$  depends on the relative mass of the organic radicals (Me, Ph or  $\text{CH}_2\text{CH}_2\text{CH}_2\text{NH}_2$ ) present in the xerogel; it was higher for **3b** and **6** containing  $\text{CH}_2\text{CH}_2\text{CH}_2\text{NH}_2$  or Ph groups and lower for **5** containing Me groups.

Note that the composition of the hydrocarbons formed on heating depends on the xerogel composition. For example, after heating to  $300^\circ\text{C}$  for 2 h, the ethane:ethylene:propane:propylene:isobutylene ratio is  $9\text{:}69\text{:}6\text{:}0\text{:}16$  or  $10\text{:}4\text{:}16\text{:}14\text{:}56$  for xerogels **3b** and **6**, respectively. The difference in the composition of the gas phases resulted from different catalytic effects of the solid pyrolysis products on the Fischer–Tropsch reaction between CO and  $\text{H}_2$  evolved in the thermal decomposition of xerogels. The composition of the crystalline phase of these solid products depends on the nature of the starting xerogel and also on the pyrolysis conditions. In all cases, amorphous silica was formed (halo for scattering angle ranges  $2\theta = 15\text{--}28^\circ$ ,  $28\text{--}32^\circ$ ,  $43\text{--}48^\circ$ , CuK $\alpha$  radiation), but the products may also contain phases of elemental cobalt in different crystalline modifications, as well as cobalt oxides or carbides (Table 2).

The heating of xerogels **5** and **6** to  $600^\circ\text{C}$  in an argon flow led to a very great increase in the surface area (Table 3). A further increase in the temperature, as well as the presence of oxygen caused agglomeration of the materials with a subsequent decrease in the surface area. Thus, we found optimum conditions for the production of porous Co-containing materials.

Transparent high-quality greyish-green sol–gel films on a glass substrate can be obtained from a mixture of **1**,  $\text{HO}(\text{SiMe}_2\text{O})_n\text{H}$  ( $n = 3\text{--}7$ ) and  $\text{PhSi}(\text{OMe})_3$  in the molar ratio 1:6:6. The sol–gel process is accompanied by complete decomposition of  $[\text{Co}(\text{CO})_4]^-$  and by the appearance of strong IR bands in the regions  $3200\text{--}3600$  and  $1300\text{--}1500\text{ cm}^{-1}$ , which are indicative of the formation of a hydroxy cobalt carbonate. The latter is homogeneously incorporated into the gel matrix as a result of the sol–gel pro-

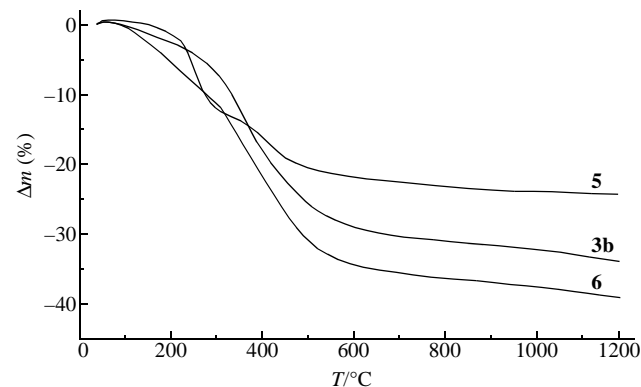


**Figure 1** TGA curves of xerogels **3b**, **5** and **6**.

cess, and the TEM images of these films exhibit the absence of any structure. Thus, the sol–gel films exhibit homogeneity and good optical properties. The absorption bands at 521, 575 and 633 nm in the visible spectrum, as well as the broad band at 1200 nm, confirm the presence of the cobalt hexamine complex incorporated into the sol–gel matrix.

This work was supported by INTAS (grant no. 97-1785), the International Centre for Advanced Studies in Nizhnii Novgorod (grant no. 98-03-3) and the Russian Foundation for Basic Research (grant no. 99-03-32911). We thank Dr. V. N. Sedelnikova and Dr. A. I. Kirillov for their assistance in analysis.

## References

- 1 I. B. Slinyakova and T. D. Denisova, *Kremniorganicheskie adsorbenty: poluchenie, svoistva i primeneniye* (Organosilicon adsorbents. Synthesis, properties and applications), Naukova Dumka, Kiev, 1988 (in Russian).
- 2 R. J. P. Corriu and D. Leclercq, *Angew. Chem., Int. Ed. Engl.*, 1996, **35**, 1420.
- 3 C. Sanchez and F. Ribot, *New J. Chem.*, 1994, **18**, 1007.
- 4 N. Husing and U. Schubert, *Angew. Chem.*, 1998, **110**, 22.
- 5 J. Fricke and T. Tillotson, *Thin Solid Films*, 1997, **297**, 212.
- 6 J. Zarzycki, *Heterogen. Chem. Rev.*, 1994, **1**, 243.
- 7 L. S. Klein, *Annu. Rev. Mater. Sci.*, 1993, **23**, 437.
- 8 D. Levy and L. Esquivias, *Adv. Mater.*, 1995, **7**, 120.
- 9 U. Schubert, *New J. Chem.*, 1994, **18**, 1049.
- 10 J. Wender, H. W. Sternberg and M. Orchin, *J. Am. Chem. Soc.*, 1952, **74**, 1216.
- 11 W. Hieber and R. Wiesboeck, *Chem. Ber.*, 1958, **91**, 1146.

*Received: 2nd November 1999; Com. 99/1549*